

# Multilayer Planar Structures for High-Directivity Directional Coupler Design

MANUEL HORNO, MEMBER, IEEE, AND FRANCISCO MEDINA

**Abstract** — One of the problems that appears in the directional couplers designed with nonhomogeneous coupled transmission lines (CTL's) is their inherently poor directivity, due to the difference between the mode phase velocities. In order to overcome this defect, several multilayer configurations for high-directivity coupler design are proposed and studied in this paper. The analysis has been achieved by means of variational techniques in the spectral domain. A computer program to generate optimum design curves has been written, and several examples for certain dielectric materials are included. On the basis of these curves, various directional coupler designs are presented and discussed.

## I. INTRODUCTION

THE GROWING COMPLEXITY of microwave integrated circuitry and the quality requirements of basic components are increasing the voltage standing-wave ratio (VSWR) and isolation of directional couplers. For edge-coupled microstrip directional couplers, the well-known even- and odd-mode theory shows different phase velocities for the even and odd modes of propagation. Broadside-coupled configurations yield much larger deviations from equality. This inequality of mode lengths resulting from the inhomogeneity of the wave propagation medium significantly affects coupler performance; for this reason, microstrip directional couplers exhibit a reduced directivity. Thus, to improve coupler directivity, the phase velocities of guided fundamental modes have to be equalized. Several methods for compensation have been proposed by different authors. The effect of an additional dielectric layer placed on the coupled line interface (overlay techniques) has been studied under the quasi-TEM assumption [1]–[3], [6] and using a full-wave analysis [4], [5], [7] for two-[1]–[5] and three-line [6], [7] couplers. Shibata *et al.* [8] showed that adjustment of air gap in suspended microstrip lines make it possible to compensate for the difference of the even- and odd-mode phase velocities. Horro *et al.* [9] proposed a two-layer configuration to improve the performance of two-line microstrip couplers, and Janiczak [10] extended the method to the three-line coupled microstrip structure. The anisotropy of the dielec-

tric substrate has also been considered for overcoming the defect of microstrip couplers [11]–[13].

In this work, on the basis of the quasi-TEM assumption, we analyze a variety of open and closed stratified configurations (with iso/anisotropic dielectrics) for edge- and broadside-coupled strips, which permit us to get equal mode phase velocities. The multiple boundary value problem involved is treated using the variational technique in the spectral domain reported in [14], which provides very accurate results in a short CPU time. For each of the analyzed structures, we show a pair of graphs for optimum design, and a set of two-line couplers have been designed and compared. Experimental data have not been included because of the unavailability of adequate equipment, but we expect to provide them at a future date.

## II. METHOD OF ANALYSIS

The inhomogeneous geometries proposed in this paper in order to improve the performance of microstrip couplers or filters are represented in Fig. 1. Fig. 1(a) and (b) represents edge-coupled microstrip configurations suitable for weak coupling, and Fig. 1(c), (d), (e), and (f) represents broadside-coupled strips, which provide strong coupling between the conductors. All of these structures preclude pure TEM mode propagation, but if cross-sectional dimensions are much smaller than the wavelength to be used, the quasi-TEM assumption is valid. Each of the geometries represented can propagate two orthogonal modes, namely the even and odd modes. The symmetry of the configurations allows us to reduce the problem to the evaluation of the electrical energy per unit length in a quarter of the cross section (the upper right quarter, for instance). In this way, our structures are particular cases of the multistratified configuration studied by the authors in [14], assuming that  $L$  [14, fig. 1] is large enough when considering structures without lateral shielding. For analysis in the spectral domain, the mode capacitances are written as follows:

$$C_{e,o} = (1/LV^2) \sum_{n=1}^{\infty} \tilde{L}(n) \cdot |\tilde{V}^m(n)|^2 \quad (1)$$

$$(1/C_{e,o}) = (1/LQ^2) \sum_{n=1}^{\infty} \tilde{G}(n) \cdot |\tilde{\rho}^m(n)|^2, \quad m = e, o \quad (2)$$

Manuscript received March 26, 1986; revised June 26, 1986. This work was supported in part by the Comisión Asesora de Investigación Científica y Técnica, Spain.

The authors are with the Departamento de Electricidad y Electrónica, Facultad de Física, Universidad de Sevilla 41012, Sevilla, Spain.

IEEE Log Number 86105557.

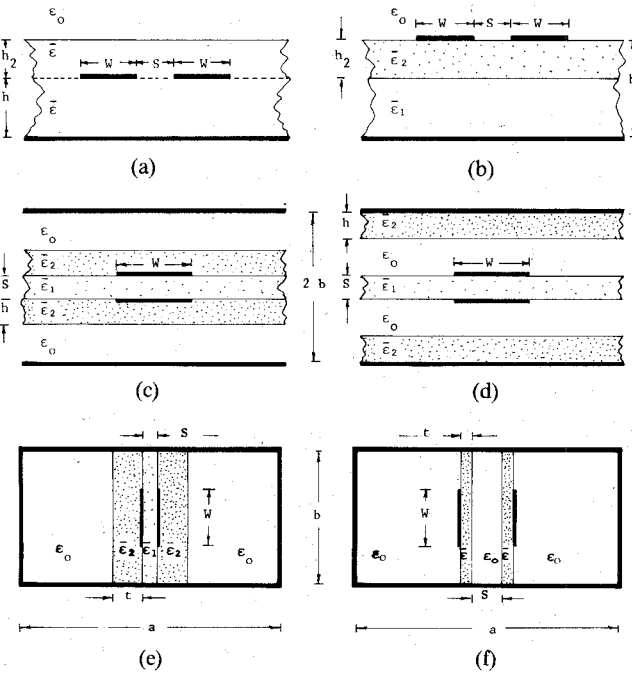


Fig. 1. Cross sections of the coupled structures analyzed in this paper. (a) Edge-coupled strips with overlay. (b) Edge-coupled strips on two substrates. (c) Broadside-coupled strips with overlay. (d) Broadside-coupled strips with two dielectrics. (e) Broadside-coupled strips with overlay in rectangular waveguide. (f) Broadside-coupled strips in rectangular waveguide with air gap.

where  $\tilde{V}^m(n)$  and  $\rho^m(n)$  are, respectively, the Fourier transforms of the potential distribution and the surface charge density at the interface where the strips are located;  $\tilde{G}(n) = \{\tilde{L}(n)\}^{-1}$  is the Green's spectral function for the structure; and  $Q$  and  $V$  are the strip charge and potential for each mode. The Green's function is determined applying the recurrence expressions which appeared in [14].

The expressions (1) and (2) are useful in calculating upper and lower bounds on mode capacitances, respectively. However, since (2) is more efficient than (1), only (2) has been used to generate numerical data in this paper. Due to the stationary nature of (2), very accurate results can be obtained using adequate trial functions to approximate  $\rho^m(x)$  on the strips. In this work, the following trial functions have been chosen.

#### a) Edge-Coupled Strips

$$\rho^m(x) = \frac{1}{w} + a_1 \cdot \left\{ \frac{1}{\sqrt{\frac{x-s/2}{w}}} - 2 \right\} + a_2 \left\{ \frac{1}{\sqrt{\frac{s/2+w-x}{w}}} - 2 \right\}, \quad \frac{s}{2} \leq x \leq \frac{s}{2} + w. \quad (3)$$

#### b) Broadside-Coupled Strips

$$\rho^m(x) = \frac{2}{w} + a_1 \cdot \left\{ \frac{1}{\sqrt{\frac{w/2-x}{w}}} - 1 \right\}, \quad 0 \leq x \leq \frac{w}{2}. \quad (4)$$

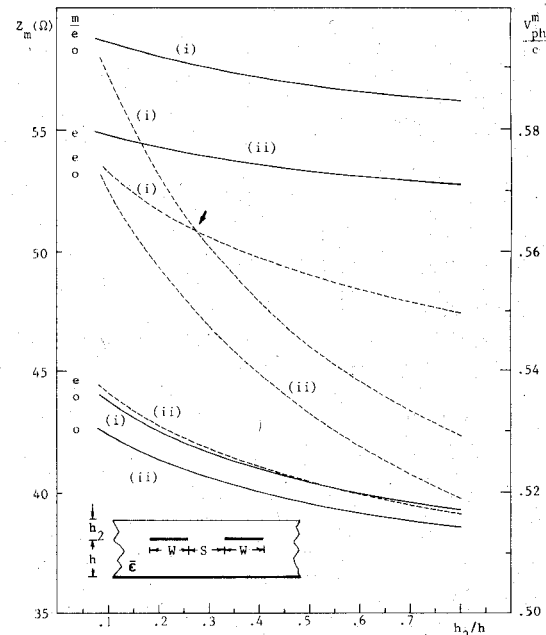


Fig. 2. Edge-coupled strips embedded in (i) P.B.N. ( $\epsilon_x^* = 5.12$ ,  $\epsilon_y^* = 3.40$ ) and (ii) isotropic dielectric with  $\epsilon^* = 4.10$  ( $= \sqrt{\epsilon_x^* \cdot \epsilon_y^*}$ ). If we vary the ratio  $h_2/h$ , mode phase velocities can be matched in case (i), but this is not possible in case (ii).  $W/h = 1.0$ ,  $S/h = 0.5$ .

The variational parameters  $a_i$  are obtained by applying the Rayleigh-Ritz minimization procedure. Note that trial functions are constructed with a constant term incorporating the total charge on the strips, and other terms (which do not contribute to the net charge) involving the edge singularities of the charge distributions.

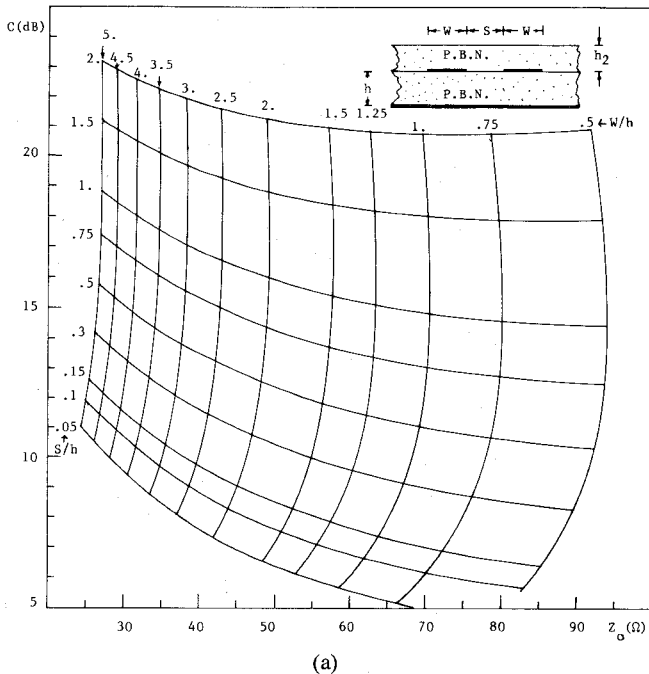
### III. ANALYSIS OF THE STRUCTURES

The method described has been used to write a computer program to analyze the configuration in Fig. 1. Upper and lower bounds on mode capacitance were generated to check the results. Agreement of better than 0.2 percent of the average value was found for practical dimensions.

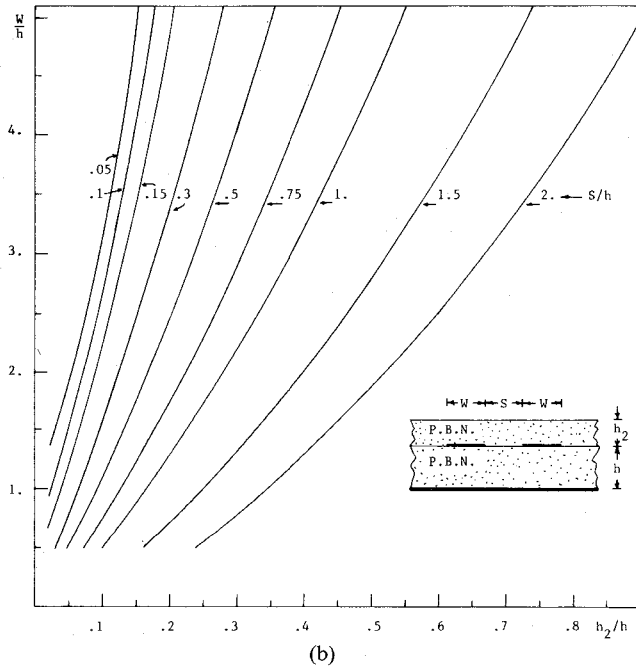
As shown in Fig. 1, these structures are obtained by modifying the simpler edge-coupled or broadside-coupled strip configurations. The addition of one dielectric layer or air gap permits us to match the even- and odd-mode phase velocities by changing its thickness. In the following paragraphs we will present a condensed study of these CTL configurations.

#### A. Edge-Coupled Lines with Overlay (Fig. 1(a))

Overlay techniques have been employed by several authors to obtain equal mode phase velocities [1]–[3]. Nevertheless, the structure here proposed is original because only one anisotropic material is needed to build the substrate and the superstrate. As shown in Fig. 2, it is possible to match the mode phase velocities by varying the thickness of the overlay if pyrolytic boron nitride (P.B.N.) is used as a low-loss dielectric ( $\epsilon_x^* = 5.12$ ,  $\epsilon_y^* = 3.40$ ). Also, it is apparent from this figure that if an equivalent isotropic dielectric is used ( $\epsilon^* = 4.1$ ), equality cannot be



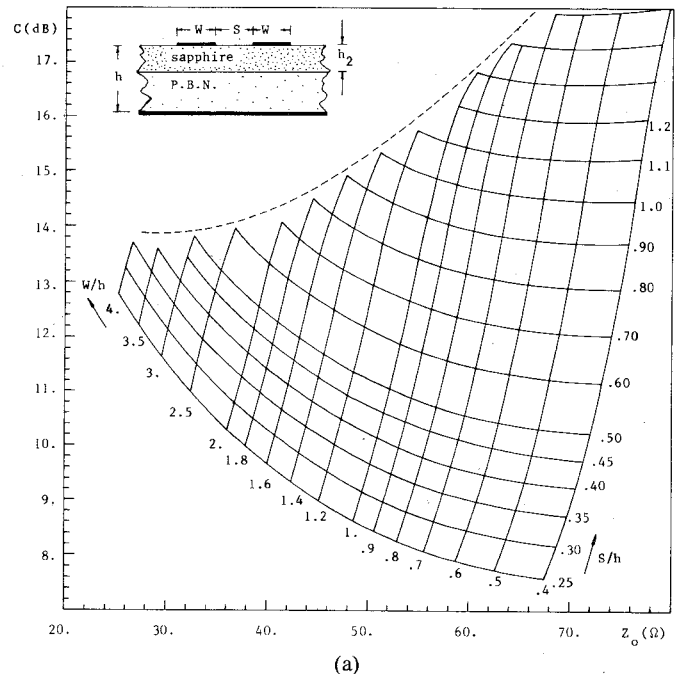
(a)



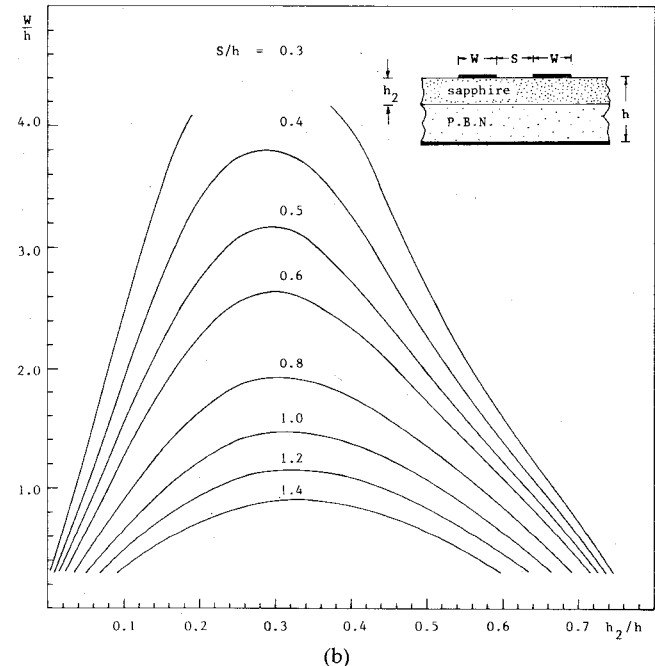
(b)

Fig. 3. Design curves for edge-coupled strips embedded in P.B.N. (a) Central frequency coupling versus characteristic impedance. (b) Optimum  $h_2/h$  ratio.

achieved (from a theoretical point of view) with an overlay of finite thickness. For each pair of values  $(W, S)$ , we find an optimum overlay thickness ( $h_2$ ) which yields equal mode phase velocities. From this, we have written a computer program to obtain the optimum shape ratios for our purposes. The results are shown in graphic form in Fig. 3. Once we have fixed the coupling at the central frequency ( $C$ (dB)) and the characteristic impedance ( $Z_0$ ) of the coupler, we can obtain the values of  $W$  and  $S$  from Fig. 3(a). Using these values in Fig. 3(b), we obtain the opti-



(a)



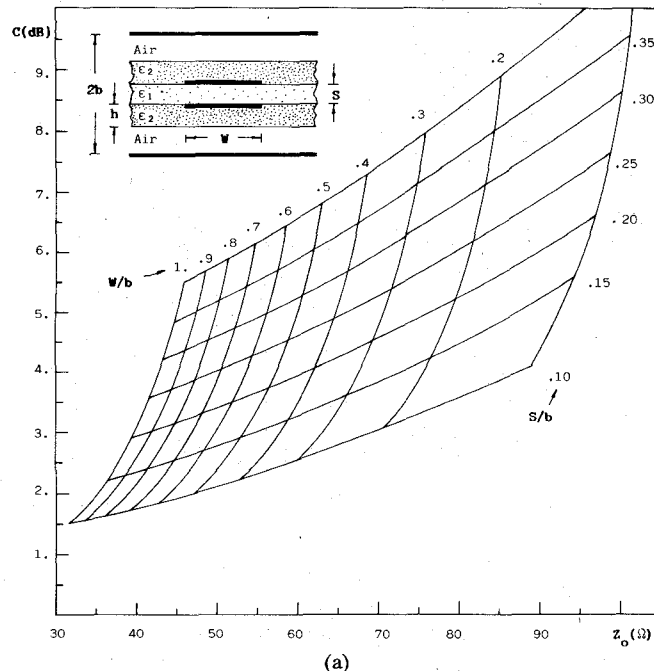
(b)

Fig. 4. Design curves for edge-coupled strips on a double-layer substrate (P.B.N.-sapphire). (a) Central-frequency coupling versus characteristic impedance. (b) Optimum  $h_2/h$  ratio. Dashed lines denote the theoretical limit of validity for the structure with this compound substrate.

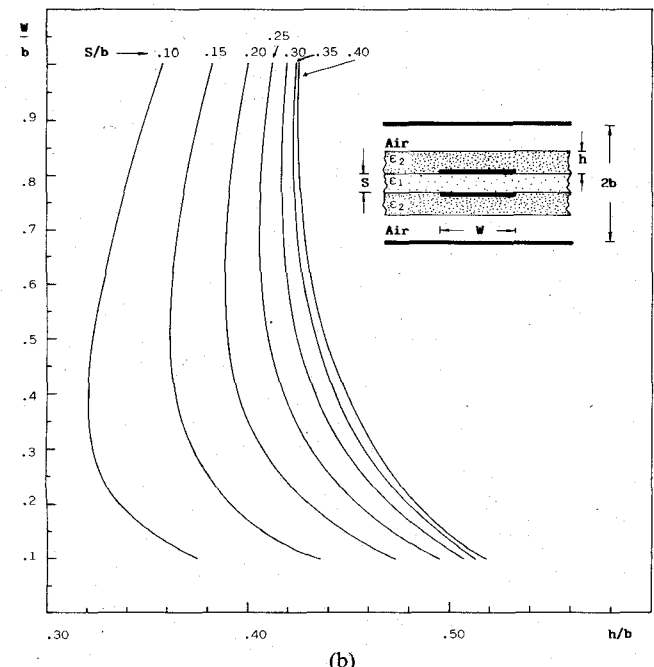
mum overlay thickness. Similar design graphs can be drawn for overlay configurations if the dielectric constant of the overlay is higher than the dielectric constant of the substrate.

#### B. Edge-Coupled Lines on Two Substrates (Fig. 1(b))

As stated in [9], we can also match the mode phase velocities by using two layers of different materials as a compound substrate. For each pair  $(W, S)$ , there are two values of the ratio  $h_2/h$  which permits us to equalize the



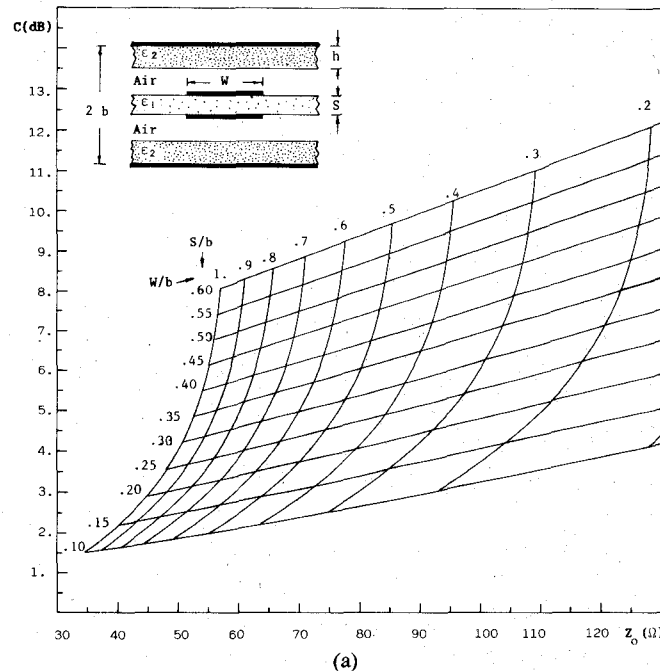
(a)



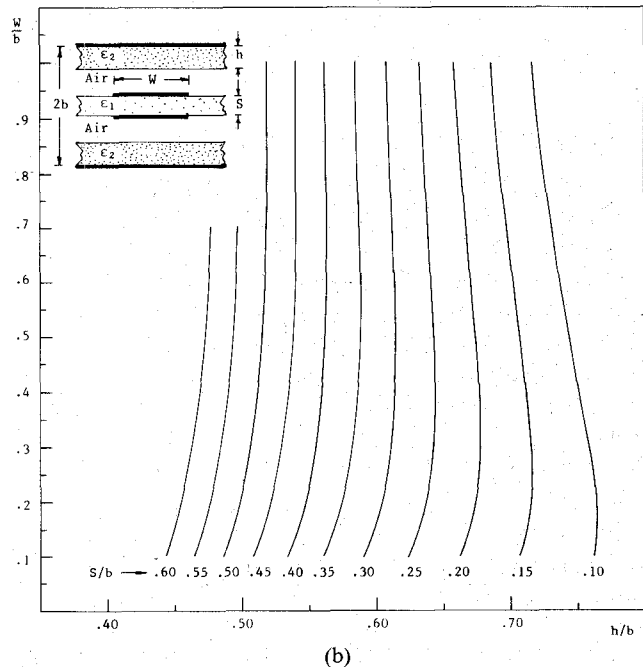
(b)

Fig. 5. Design curves for broadside-coupled strips with overlay ( $\epsilon_1^* = 2.5$ ,  $\epsilon_2^* = 10.0$ ). (a) Central-frequency coupling versus characteristic impedance. (b) Optimum  $h/b$  ratio.

even- and odd-mode phase velocities. Obviously, the coupling factor is the same for both matching points, but the characteristic impedance is different. If we proceed as in Section III-A, two different graphs of  $C(\text{dB})$  versus  $Z_0$  can be drawn. However, we only present (see Fig. 4(a)) the graph for the higher value of  $h_2/h$  here, because when using the chosen dielectric materials (sapphire and boron nitride) this value yields suitable impedance levels. Once we decide the required values of  $Z$  and  $C(\text{dB})$ , we use this graph to determine the pair  $(W, S)$ , and the optimum



(a)



(b)

Fig. 6. Design curves for broadside-coupled strips with two substrates ( $\epsilon_1^* = 2.5$ ,  $\epsilon_2^* = 10.0$ ). (a) Central-frequency coupling versus characteristic impedance. (b) Optimum  $h/b$  ratio.

$h_2/h$  is directly obtained from Fig. 4(b) (there are two possible values of  $h_2/h$ , but in this case, we must choose the higher). This structure can be useful in avoiding the problem of air bubbles that the overlay configuration presents. It must be noted that perfect matching can only be reached for a limited  $(W, S)$  region; therefore (with the materials proposed), it is not possible to achieve lower couplings and perfect directivity. Nevertheless, similar design curves can be easily obtained for other materials, thus avoiding this limitation.

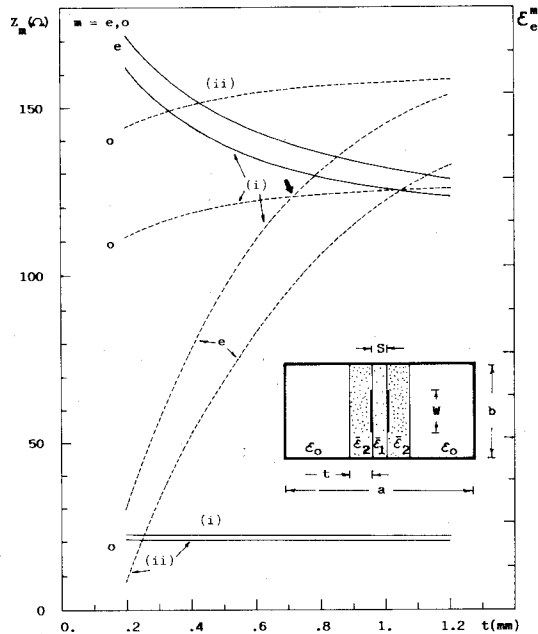


Fig. 7. Mode impedances and effective dielectric constants for broadside-coupled lines suspended in  $E$ -plane of WR-28 waveguide ( $a = 7.11$  mm,  $b = 3.56$  mm) versus overlay thickness ( $\bar{\epsilon}_1 = \bar{\epsilon}_2 = \bar{\epsilon}$ ). (i) P.B.N. ( $\epsilon_x^* = 5.12$ ,  $\epsilon_y^* = 3.40$ ). (ii) Equivalent isotropic dielectric material ( $\epsilon_r^* = \sqrt{\epsilon_x^* \cdot \epsilon_y^*} \approx 4.10$ ).  $W = 0.8$  mm,  $S = 0.25$  mm.

### C. Broadside-Coupled Strips with Overlay (Fig. 1(c))

Conventional broadside-coupled transmission lines in a nonhomogeneous medium yield considerably different mode phase velocities, but in spite of this, they can still be highly useful in designing directional couplers and filters at lower microwave frequencies. However, to design high-directivity backward-wave directional couplers, mode phase velocities must be close again. Equalization of mode lengths can be attained using a high-permittivity overlay (see Fig. 1(c)), as stated in [15]. This configuration is similar to the one studied in Section III-A, but it allows us to get very strong coupling with practical dimensions. A pair of graphs similar to the ones above is also supplied in Fig. 5(a) and (b). These curves are used in the same way as the previous ones.

### D. Broadside-Coupled Strips with Two Layers (Fig. 1(d))

This is an alternative configuration to the one described in Section III-C. In this structure, there is an air gap between the dielectric layers, and air bubbles between them are no longer a problem. In [15], we prove that by varying the thickness of the high-permittivity substrate, mode phase velocities can be equalized. In Fig. 6(a) and (b), the corresponding design curves are represented.

### E. Broadside-Coupled Strips with Overlay in Rectangular Waveguide (Fig. 1(e))

Often, broadside-coupled structures are mounted into a rectangular waveguide such as is shown in Fig. 1(e). The proximity of the lateral electric walls allows us to match the mode effective dielectric constants by using a dielectric overlay with lower permittivity than in the dielectric used

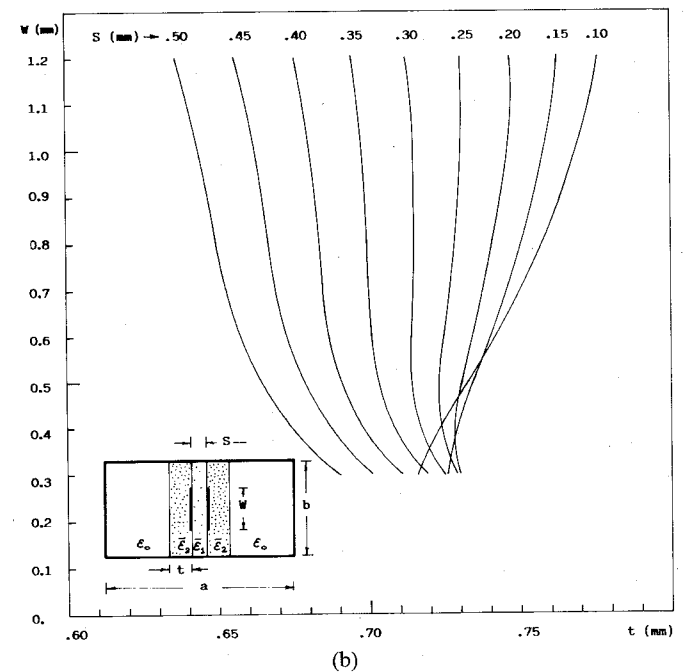
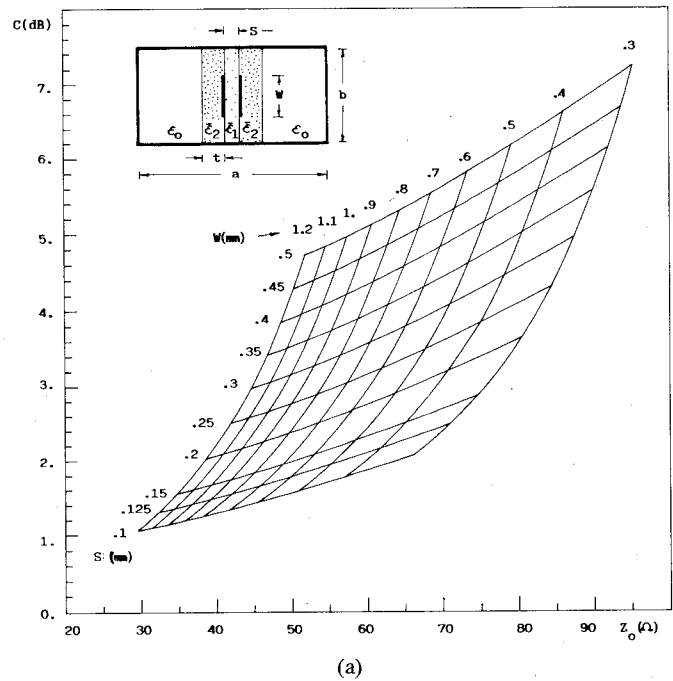


Fig. 8. Design curves for broadside-coupled strips suspended in  $E$ -plane of WR-28 waveguide with anisotropic dielectric overlay and substrate ( $\epsilon_{x_1}^* = \epsilon_{x_2}^* = 5.12$ ,  $\epsilon_{y_1}^* = \epsilon_{y_2}^* = 3.40$ ). (a) Central-frequency coupling versus characteristic impedance. (b) Optimum thickness ( $t$ ).

in the structure in Fig. 1(c). In fact, as can be seen in Fig. 7, it is possible to attain equality using only one anisotropic material, such as P.B.N. (this is not possible with an equivalent isotropic material). Design curves for broadside-coupled strips with overlay in the  $E$ -plane of WR-28 waveguide are shown in Fig. 8.

### F. Broadside-Coupled Strips in Rectangular Waveguide with Air Gap (Fig. 1(f))

In this geometry, the equalization is achieved by adjusting the air gap between the high-permittivity dielectric

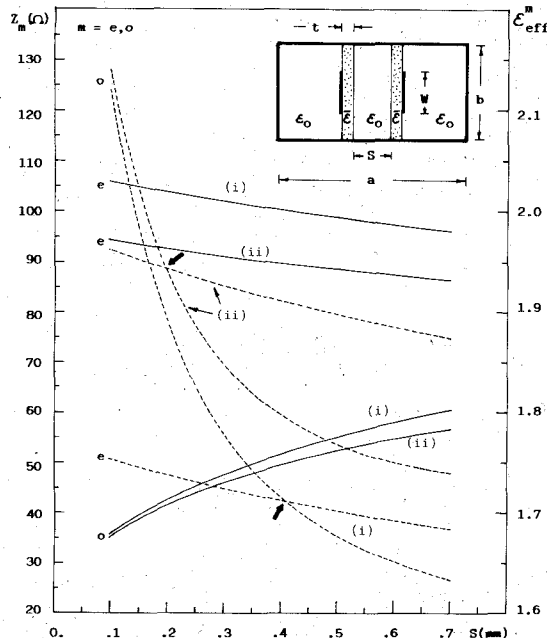


Fig. 9. Mode impedances and effective dielectric constants for broadside-coupled lines suspended in  $E$ -plane of WR-28 waveguide ( $a = 7.11$  mm,  $b = 3.56$  mm) versus air gap ( $S$ ). (i) Sapphire ( $\epsilon_x^* = 9.40, \epsilon_y^* = 11.60$ ). (ii) Epsilam-10 ( $\epsilon_x^* = 13.0, \epsilon_y^* = 10.2$ ).  $W = 1.0$  mm,  $t = 0.35$  mm.

layers. In Fig. 9, we show the effect of the air gap on the propagation characteristics for sapphire and Epsilam-10. Effective dielectric constant matching is emphasized in the picture with arrows. The corresponding design curves for sapphire substrate are shown in Fig. 10.

#### IV. RESULTS

Making use of the design graphs discussed above, several 3-dB, 6-dB, 10-dB, and 20-dB 50-Ω couplers have been designed. The calculated center-frequency coupling, directivity, and VSWR of six coupler designs are presented in Table I, together with their dimensions, impedances, and phase velocities. In Fig. 11, we can see the effect on central-frequency directivity, characteristic impedance, and coupling of errors or lack of precision (due to the tolerances) in the thickness of the added layer ( $h_2, h, t$ ) or air gap ( $S$ ). Coupler no. 1 is a 20-dB, 50-Ω microstrip coupler on P.B.N. with P.B.N. overlay. Note from Fig. 11 that if  $h_2/h = 0.5$  or 0.4, directivity remains over 30 dB while coupling and characteristic impedance are practically unchanged with regard to the optimum  $h_2/h$  ratio ( $h_2/h = 0.45$ ), indicating that phase velocity mismatch will not be the dominant factor in limiting coupler performance even if the overlay thickness differs from the optimum value by 10 percent. Similar comments can be applied to the 10-dB, 50-Ω coupler denoted in Table I with the number 2. Couplers 3, 4, and 5 are 3-dB, 50-Ω couplers with very high directivity, but VSWR and coupling are more sensitive to errors in the choice of the thickness of the added dielectric. In coupler 6 (6-dB, 50-Ω) the air gap must be carefully chosen because of its sensitivity to errors in it.

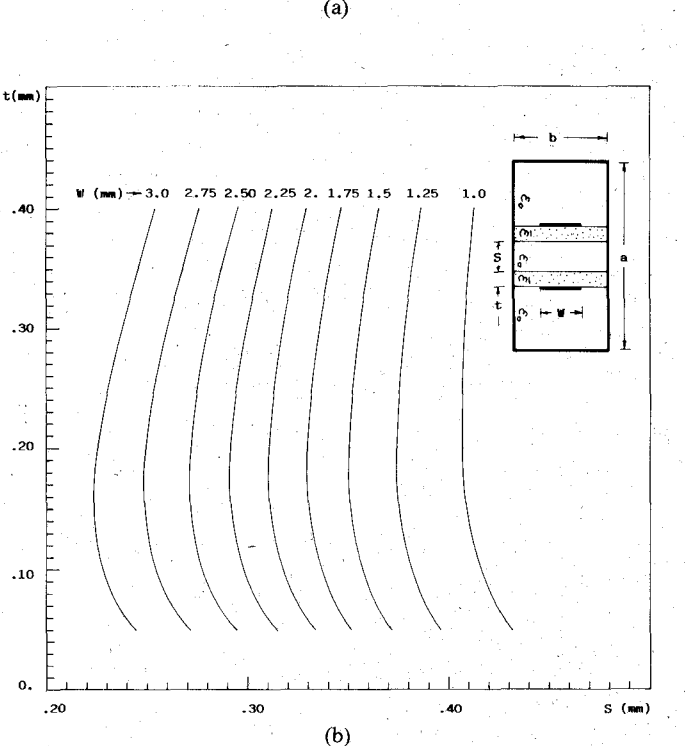
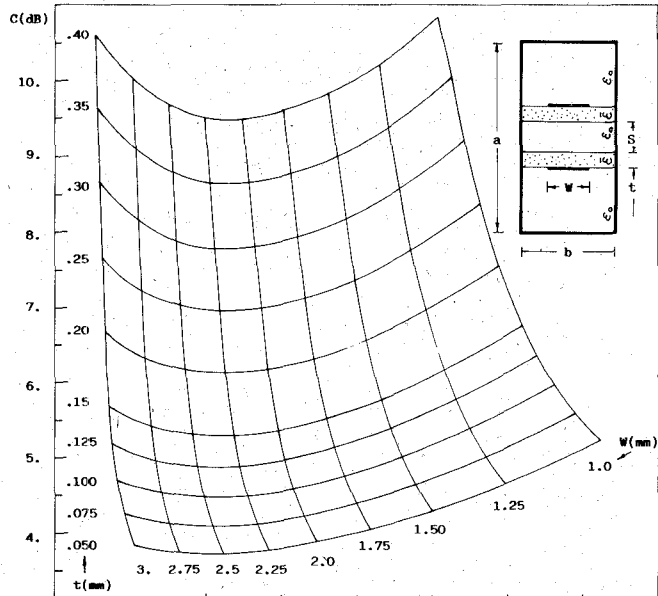


Fig. 10. Design curves for broadside-coupled strips suspended in  $E$ -plane of WR-28 waveguide with sapphire dielectric ( $\epsilon_x^* = 9.40, \epsilon_y^* = 11.60$ ). (a) Central-frequency coupling versus characteristic impedance. (b) Optimum air gap ( $S$ ).

#### V. CONCLUSIONS

The variational approach in the spectral domain is a powerful tool in analyzing the propagation parameters of multilayered configurations under quasi-TEM assumption. This method has been used in this paper to study a set of simple coupled configurations which can be useful in the design of high-directivity directional couplers. It has been shown that the addition of one iso/anisotropic dielectric layer makes it possible to improve substantially the direc-

TABLE I  
COUPLER DESIGNS USING THE STRUCTURES IN FIG. 1

No.	Struct.	TYPE	DIMENSIONS	Dir			
				$Z_0$ ( $\Omega$ )	C (dB)	(dBs)	SWR
1	(a)	20 dB	$W/h=1.93$ , $S/h=1.75$ $h_2/h=0.45$	49.94	20.03	58.00	1.003
2	(b)	10 dB	$W/h=1.04$ , $S/h=0.38$ $h_2/h=0.65$	50.06	10.02	53.13	1.002
3	(c)	3 dB	$W/b=0.60$ , $S/b=0.17$ $h/b=0.37$	50.01	3.01	54.70	1.003
4	(d)	3 dB	$W/b=0.85$ , $S/b=0.20$ $h/b=0.66$	50.34	3.06	54.70	1.003
5	(e)	3 dB	$W=0.95$ mm, $S=0.28$ mm $t=0.70$ mm	50.30	3.02	61.00	1.002
6	(f)	6 dB	$W=1.85$ mm, $t=0.22$ mm $S=.29$ mm	50.20	6.25	56.00	1.001

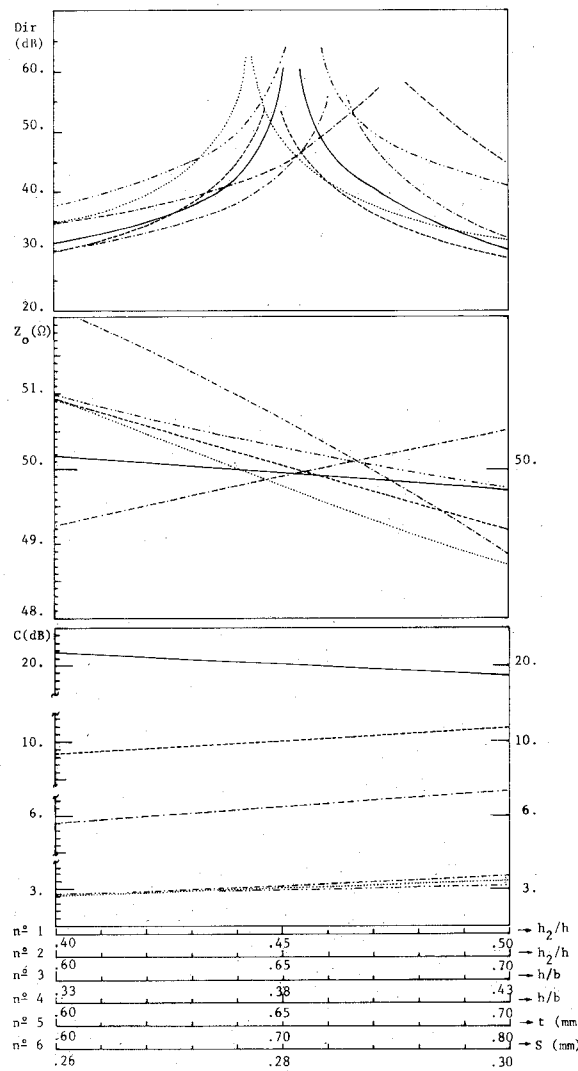


Fig. 11. Central-frequency directivity, characteristic impedance, and coupling versus thickness of the added dielectric layer (1-5) or air gap (6). This figure refers to the coupler designs presented in Table I. — coupler no. 1. - - - coupler no. 2. ····· coupler no. 3. - - - - coupler no. 4. - - - - - coupler no. 5. - - - - - - coupler no. 6 (scaling for the bottom graph (coupling,  $C$ ) is 0.1 dB per division).

tivity of inherently poor coupler structures. A set of computer programs has been written to provide optimum design curves for each of the structures presented in the work. By making use of these graphs, several high-performance coupler designs have been achieved. Also, the influence of dimensional tolerances of the added dielectric layer or air gap has been considered. It has been shown that optimum designs are not critical because significant deviations from optimum values still lead to high-quality theoretical performance in such a way that phase velocity mismatch is not the dominant degrading factor.

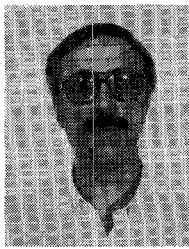
## REFERENCES

- [1] G. Haupt and H. Delfs, "High-directivity microstrip directional couplers," *Electron Lett.*, vol. 10, no. 9, pp. 142-143, May 1974.
- [2] D. D. Paolino, "MIC overlay coupler design using spectral domain techniques," *IEEE Trans. Microwave Theory Tech.*, vol. MTT-26, pp. 646-649, Sept. 1978.
- [3] N. G. Alexopoulos and S. A. Maas, "Performance of microstrip couplers on an anisotropic substrate with an isotropic superstrate," *IEEE Trans. Microwave Theory Tech.*, vol. MTT-31, pp. 671-674, Aug. 1983.
- [4] K. Shibata and K. Hatori, "Dispersion characteristics of coupled microstrip with overlay on anisotropic dielectric substrate," *Electron. Lett.*, vol. 20, no. 1, pp. 19-20, Jan. 1984.
- [5] L. Suo, T. Itoh, and J. Rivera, "Design of an overlay directional coupler by a full-wave analysis," *IEEE Trans. Microwave Theory Tech.*, vol. MTT-31, pp. 1017-1022, Dec. 1983.
- [6] K. Shibata, H. Yanagisawa, and Y. Ishihata, "Three-line microstrip directional coupler with dielectric overlay," *Electron. Lett.*, vol. 19, no. 22, pp. 911-912, Oct. 1983.
- [7] B. J. Janiczkak, "Accurate hybrid-mode approach for computing modes in three-line coupled microstrip structure in overlaid configuration," *Electron. Lett.*, vol. 20, no. 20, pp. 825-826, Sept. 1984.
- [8] K. Shibata, H. Yanagisawa, Y. Torimura, and K. Hatori, "Method for improving microstrip coupler directivity," *Electron. Lett.*, vol. 17, no. 20, pp. 732-733, Oct. 1981.
- [9] M. Horro and R. Marques, "Coupled microstrips on double anisotropic layers," *IEEE Trans. Microwave Theory Tech.*, vol. MTT-32, pp. 467-471, Apr. 1984.
- [10] B. J. Janiczkak, "Phase velocity compensation in three-line coupled microstrip structure by using stratified dielectric substrate," *Electron. Lett.*, vol. 21, no. 4, pp. 145-146, Feb. 1985.
- [11] N. G. Alexopoulos, S. Kerner, and C. M. Krowne, "Dispersionless coupled microstrips over fused silica-like anisotropic substrates," *Electron. Lett.*, vol. 12, no. 22, pp. 579-580, Oct. 1976.

- [12] M. Kobayashi and R. Terakado, "Method for equalizing phase velocities of coupled microstrip lines by using anisotropic substrate," *IEEE Trans. Microwave Theory Tech.*, vol. MTT-28, pp. 719-722, July 1980.
- [13] N. G. Alexopoulos and S. A. Maas, "Characteristics of microstrip directional couplers on anisotropic substrates," *IEEE Trans. Microwave Theory Tech.*, vol. MTT-30, pp. 1267-1270, Aug. 1982.
- [14] F. Medina and M. Horro, "Upper and lower bounds on mode capacitances for a large class of anisotropic multilayered microstrip-like transmission lines," *Proc. Inst. Elec. Eng., Microwaves, Optics and Antennas*, vol. 132, pt. H, pp. 157-163, July 1985.
- [15] M. Horro and F. Medina, "Accurate approach for computing quasi-static parameters of symmetrical broadside-coupled microstrips in multilayered anisotropic dielectrics," *IEEE Trans. Microwave Theory Tech.*, vol. MTT-34, pp. 729-733, June 1986.

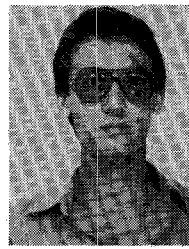
†

**Manuel Horro** (M'75) was born in Torre del Campo, Spain, on June 19, 1947. He received the degree of Licenciado in physics in June 1969 and the degree of Doctor en Ciencias in physics in January 1972, both from the University of Seville, Spain.



Since October 1969, he has been with the Department of Electricity and Electronics at the University of Seville, where he became an Assistant Professor in 1970, Associate Professor in 1975, and Titular Professor in electricity and magnetism. His main fields of interest include boundary-value problems in electromagnetic theory, wave propagation through anisotropic media, and microwave integrated circuits. He is presently engaged in the analysis of planar transmission lines embedded in anisotropic materials.

†



**Francisco Medina** was born in Puerto Real, Spain, on November 9, 1960. He received the Licenciatura degree in physics from the University of Seville, Spain, in September 1983.

He is currently Assistant Professor of electricity and magnetism at the Department of Electricity and Electronics, University of Seville, where he is now studying for the Ph.D. degree. His current interests are in multiconductor planar transmission lines and MIC design.